Conference materials
UDC 535.3
DOI: https://doi.org/10.18721/JPM/161.317

Interband photoluminescence of InAs(P)/Si nanowires

R.V. Ustimenko [1]✉, M.Ya. Vinnichenko [1], D.A. Karaulov [1], D.A. Firsov [1],
V.V. Fedorov [1,2], A.M. Mozharov [2], D.A. Kirilenko [3,4], I.S. Mukhin [1,2]

[1] Peter the Great St. Petersburg Polytechnic University, St. Petersburg, Russia;
[2] Alferov University, St. Petersburg, Russia;
[3] ITMO University, St. Petersburg, Russia;
[4] Ioffe Institute, St. Petersburg, Russia;
✉ ratmirustimenko@yandex.ru

Abstract. Semiconductor nanowires have a number of advantages over thin films and bulk analogues, which allow them to be used to develop efficient detectors and light sources. In this work, photoluminescence spectra of pure InAs and core-shell InAs/CaF_2 and InAs/InP nanowires on silicon were studied in the near infrared spectral range at various levels of optical pumping and at different temperatures using a vacuum Fourier spectrometer operating in a step-scan mode. The observed peaks in the photoluminescence spectra correspond to interband transitions in InAs of sphalerite and wurtzite phases. The photoluminescence spectra of CaF_2-coated InAs nanowires demonstrated that surface passivation with CaF_2 does not change the spectral features. It was shown that the absolute value of photoluminescence intensity of InAs-core/InP-shell nanowires exceeds the intensity of pure InAs nanowires. It means that surface passivation can reduce an effect of surface states in nanowires on their optical properties.

Keywords: nanowires, passivation, photoluminescence, core/shell nanowires

Funding: This work was supported by the Russian Science Foundation (grant № 22-19-00494, https://rscf.ru/en/project/22-19-00494/).

Citation: Ustimenko R.V., Vinnichenko M.Ya., Karaulov D.A., Firsov D.A., Fedorov V.V., Mozharov A.M., Kirilenko D.A., Mukhin I.S., Interband photoluminescence of InAs(P)/Si nanowires, St. Petersburg State Polytechnical University Journal. Physics and Mathematics. 16 (1.3) (2023) 101–107. DOI: https://doi.org/10.18721/JPM.161.317

This is an open access article under the CC BY-NC 4.0 license (https://creativecommons.org/licenses/by-nc/4.0/)

Материалы конференции
УДК 535.3
DOI: https://doi.org/10.18721/JPM/161.317

Межзонная фотолюминесценция нитевидных нанокристаллов InAs(P)/Si

Р.В. Устименко [1]✉, М.Я. Винниченко [1], Д.А. Караулов [1], Д.А. Фирсов [1],
В.В. Фёдоров [1,2], А.М. Можаров [2], Д.А. Кириленко [3,4], И.С. Мухин [1,2]

[1] Санкт-Петербургский политехнический университет Петра Великого, Санкт-Петербург, Россия;
[2] Алфёровский Университет, Санкт-Петербург, Россия;
[3] Университет ИТМО, Санкт-Петербург, Россия;
[4] Физико-технический институт им. А.Ф. Иоффе РАН, Санкт-Петербург, Россия
✉ ratmirustimenko@yandex.ru

Аннотация. Нитевидные полупроводниковые нанокристаллы имеют ряд преимуществ по сравнению с пленками и объемными полупроводниковыми материалами, которые позволяют использовать их для создания эффективных детекторов и источников

© Ustimenko R.V., Vinnichenko M.Ya., Karaulov D.A., Firsov D.A., Fedorov V.V., Mozharov A.M., Kirilenko D.A., Mukhin I.S., 2023. Published by Peter the Great St. Petersburg Polytechnic University.

излучения. В настоящей работе были получены спектры фотолюминесценции радиально гетероструктурированных нитевидных нанокристаллов InAs, InAs/CaF_2 и InAs/InP (ядро/оболочка) в ближнем инфракрасном диапазоне при различных уровнях оптической накачки и различных температурах при помощи вакуумного фурье-спектрометра, работающего в пошаговом режиме. Обнаруженные в спектрах пики объяснены межзонными переходами носителей заряда в InAs разной кристаллической модификации: сфалерит и вюрцит. Из спектров нитевидных нанокристаллов, покрытых CaF_2, видно, что в этом случае пассивация поверхности не изменяет спектральные особенности люминесценции. В то же время интенсивность фотолюминесценции нитевидных нанокристаллов InAs/InP больше, чем у чистых нитевидных нанокристаллов InAs. Таким образом, поверхностная пассивация может уменьшить влияние поверхностных состояний на оптические свойства нитевидных нанокристаллов.

Ключевые слова: нитевидные нанокристаллы, пассивация поверхности, фотолюминесценция, нитевидные нанокристаллы ядро/оболочка

Финансирование: Исследование выполнено за счет гранта Российского научного фонда № 22-19-00494, https://rscf.ru/project/22-19-00494/.

Ссылка при цитировании: Устименко Р.В., Винниченко М.Я., Караулов Д.А., Фирсов Д.А., Фёдоров В.В., Можаров А.М., Кириленко Д.А., Мухин И.С. Межзонная фотолюминесценция нитевидных нанокристаллов InAs(P)/Si // Научно-технические ведомости СПбГПУ. Физико-математические науки. 2023. Т. 16. № 1.3. С. 101–107. DOI: https://doi.org/10.18721/ JPM.161.317

Статья открытого доступа, распространяемая по лицензии CC BY-NC 4.0 (https://creativecommons.org/licenses/by-nc/4.0/)

Introduction

Nanowires (NWs) based on A3B5 semiconductors have great prospects as a nanoscale platform for efficient electronic devices. The development of light-emitting and photo-converting devices based on NWs is a promising and urgent task [1]. NWs, due to their small lateral size and small area of contact with the substrate, have some significant advantages over films and bulk materials. They can be directly grown on various substrates, for example, silicon [2]. Thus, it is possible to produce cheap devices integrated with the silicon industrial platform. Among other A3B5 semiconductors, InAs NWs have a number of advantages owing to high mobility, low effective electron mass, low band gap *Eg* and high spin-orbit interaction energy. Also, the interest in the creation of InAs NWs is caused by the fact that selecting appropriate size of NWs can lead to the manifestation of waveguide properties and optical resonances (whispering gallery modes, Fabry-Perot and Mi resonances) in the visible and near-IR spectral ranges, which ensure the localization and concentration of light inside the NW. In this case, it is possible to achieve effective absorption of radiation in a small volume of the active region, which should reduce the dark current of optoelectronic devices. Surface passivation efficiently eliminates surface states in NWs [3]. Due to the high surface-to-volume ratio, it has a significant effect on the optical properties of NWs [4]. Light emission related to surface states of core/shell NWs can appear at photon energy greater or less than the energy of band gap of InAs NWs and can greatly reduce the luminescence efficiency. For InAs NWs, such states have a more essential effect on the emission intensity due to narrow *Eg* and significant contribution of Auger processes [5].

It is known that *Eg* of InAs-based NWs is larger than in the bulk material [6-8]. Therefore, the currently achieved sensitivity of existing detectors based on InAs NWs is limited by 3 μm wavelength, which is noticeably shorter than the experimentally observed cutoff wavelengths for InAs thin-film photodetectors (~3.8 μm). Moreover, there are several unresolved problems in creation of InAs NWs-based photodetectors. For example, the photodiodes described in the literature have a large dark current exceeding 130 mA/cm^2 [9, 10]. The effect of passivation of InAs NWs with a wider gap InP, as well as heterostructures of the *n*-InP/*i*-InAs/*p*-Si type, has not been studied in details yet. We report on optical characterization of such NWs, which can be used for developing new infrared photodetectors.

© Устименко Р.В., Винниченко М.Я., Караулов Д.А., Фирсов Д.А., Фёдоров В.В., Можаров А.М., Кириленко Д.А., Мухин И.С., 2023. Издатель: Санкт-Петербургский политехнический университет Петра Великого.

Materials and Experimental setup

Several arrays of InAs NWs were grown by means of solid-source molecular beam epitaxy (MBE) on SiO_x/Si(111) substrates within the self-induced approach. Boron-doped, vicinal *p*-type Si wafers were used (misorientation 4°, 0.3–0.5 Ohm×cm). Silicon surface oxide layer providing NW nucleation was prepared on HF-dipped Si by wet chemical oxidation in a boiling ammonia-peroxide solution (NH_4OH:H_2O_2:H_2O with a volume ratio of 1:1:3). Indium, As_4 and P_2 element fluxes were determined from beam equivalent pressures (BEP) measured by Bayard-Alpert ion gauge. For all the samples, the In flux was set to a BEP of 8×10^{-8} Torr, which corresponds to a growth rate of approximately 150 nm/h. The InAs NWs were formed at the growth temperature T_{gr} of 460 °C and a high incident As_4/In BEP flux ratio of 90, which exceeded the stoichiometric value by 5 times. To form a radial InAs-core/InP-shell heterostructure, InP was grown at the reduced T_{gr} of 400 °C and P_2/In BEP flux ratio of 32 promoting radial growth. Uniform deposition of amorphous CaF_2 was obtained at the T_{gr} of 100 °C.

Typical scanning electron microscope (SEM) image of cleaved Si substrate with pure InAs NWs is shown in Fig. 1, *a*. This morphology is typical for all studied NWs. The feature of this synthesis method is the possibility of achieving a high surface density of NWs ($\geq$10 μm^{-2}), which significantly reduces light scattering and manifests itself in the matte black surface of the sample. Depending on the growth time, the length of NWs can vary from 200 nm to 10 μm, and the diameter can vary from 40 to 300 nm. The average diameter of pure InAs NWs is approximately equal to 160 nm, their length is about 2.5 μm. We also fabricated a number of samples with surface passivation having the structure of InAs-core/InP-shell and InAs-core/CaF_2-shell. SEM image of InAs-core/InP-shell NWs is presented in Fig. 1, *b*. The diameter of InAs-core/InP-shell NWs lies in the range from 130 to 250 nm for different samples, their length is about 2.5–4.5 μm.

a) *b*)

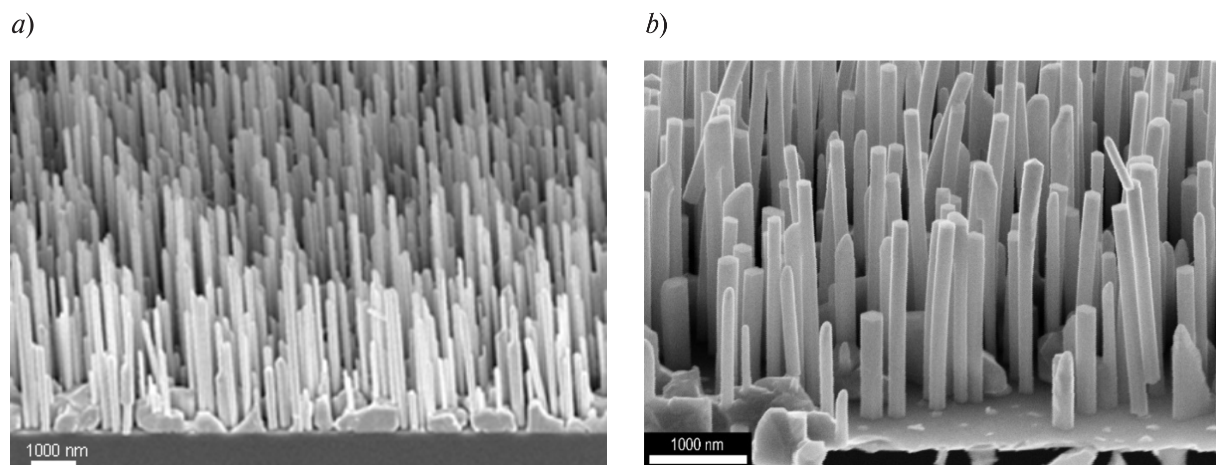

Fig. 1. SEM image of pure InAs NWs (*a*) and InAs-core/InP-shell NWs (*b*)

The crystal structure of NWs was studied by means of transmission electron microscopy (TEM) and electron microdiffraction (see Fig. 2). NWs have a hexagonal wurtzite structure; the NW growth axis coincides with the [0001] wurtzite axis. A large number of planar basal stacking fault are observed in NWs, and these defects can be of several types. Defects can be represented as inclusions of 1, 2 or 3 bi-layers of the sphalerite structure, inclusions of the cubic phase. All stacking faults are parallel to the (0001) growth plane. No other defects, for example, associated with the coalescence of neighboring NWs, were found. The electron microdiffraction pattern shows a characteristic broadening of reflections in the direction perpendicular to the plane of the defect.

Photoluminescence (PL) spectra were measured with a vacuum Fourier spectrometer operating in the step-scan mode with a spectral resolution of about 8 meV. We used the continuous wave (CW) laser radiation from a Nd:YAG solid-state laser for optical interband pumping of charge carriers in the samples. The pump radiation wavelength was 1064 nm. Nd:YAG solid-state laser was pumping by red diodes, therefore we cut this interfering light by IKS3 optical filter mounted

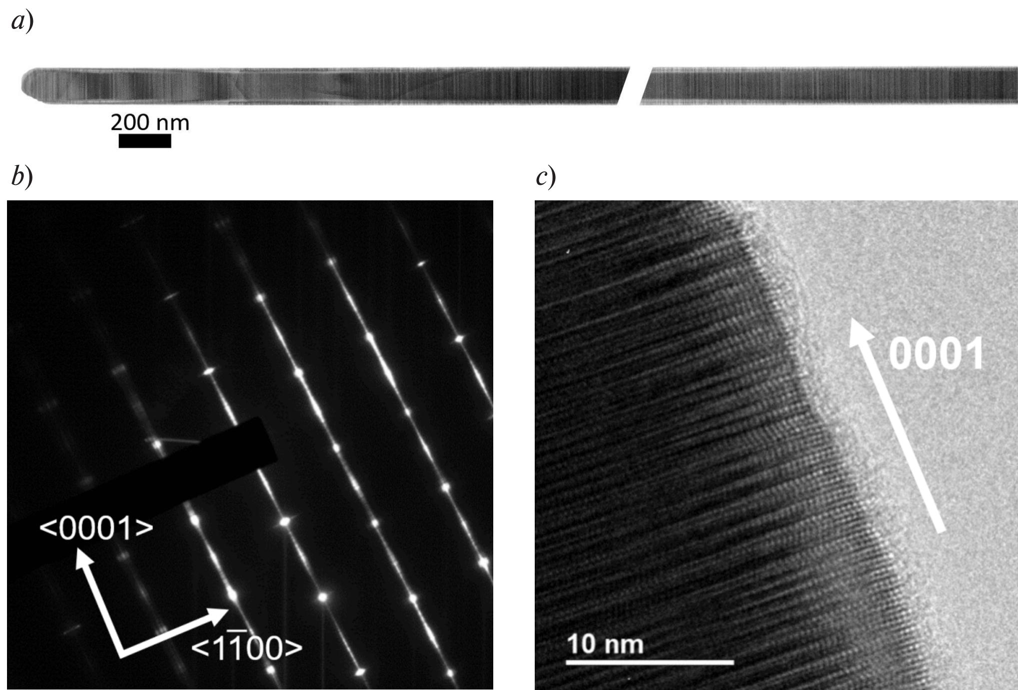

Fig. 2. TEM image of InAs-core / InP-shell NWs (*a*). Selected-area (electron) diffraction image along (*a*) <11$\bar{2}$0> WZ zone axes (*b*) and TEM image of InAs-core / InP-shell NWs (*c*)

in the optical bench. Laser radiation was modulated with a chopper at a frequency of 340 Hz and focused on the sample surface with a lens through a fused silica window of a bath cryostat. PL radiation from the sample was extracted from the cryostat through a ZnSe window aligned with the spectrometer ZnSe window. A KBr beam splitter and a liquid nitrogen-cooled InSb photodetector were used. The optical filter made from pure Ge was installed in front of the photodetector to prevent pumping radiation scattered from the sample surface to reach the detector. Samples were mounted by clamping holder on the cold copper finger of bath cryostat with liquid nitrogen. Platinum temperature controller was mounted near the sample. We varied a sample temperature from 77 to 300 K. In order to increase the measurement sensitivity, we used a phase-sensitive lock-in amplifier SR-830 synchronized with the chopper frequency.

Results and Discussion

Photoluminescence spectra were obtained in the near infrared (IR) range at different levels of optical pumping and different temperatures (77–300 K). All samples exhibited two or three PL peaks in the photon energy range from 300 to 550 meV.

PL spectra of pure InAs NWs are presented in Fig. 3, *a* for different pumping levels at the temperature of liquid nitrogen. Fig. 3, *b* shows similar results for the thinner pure InAs NWs with low surface concentration. The shape and spectral position of the peaks in these two samples are the same, but the PL intensity of peaks was significantly lower for thinner pure InAs. The increase of the sample temperature leads to a gradual quenching of the PL intensity. To analyze the PL spectra, they were fitted into three Gaussian contours (due to the inhomogeneous broadening of the PL peaks). Gaussian contours and their sum are presented as dash lines in Fig. 3, *a*. After fitting, three peaks were found at the photon energies of 350, 405, 440 meV. Two high energy peaks are associated with direct interband transitions in zincblende and wurtzite phases of InAs NWs [11]. Low-energy peak corresponds to indirect in real-space transitions in NWs between regions of the zincblende and wurtzite phases, which have different Eg [12]. It should be noted that the presence of alternating crystal modifications is confirmed by TEM images (see Fig. 2). Also, small inserts of zincblende phase could be considered as quantum wells in the wideband wurtzite phase. This can lead to additional localization of charge carriers at the heterointerfaces. The validity of our assumption is confirmed by the absence of peak energy shifts with increasing of pumping. Similar results were presented in Ref. [12], however, in

that case the peak associated with interband transitions experiences a significant blue shift with pumping increase which is opposed to our results. Also, the spectra presented in [12] contained the peak associated with donor-acceptor transitions.

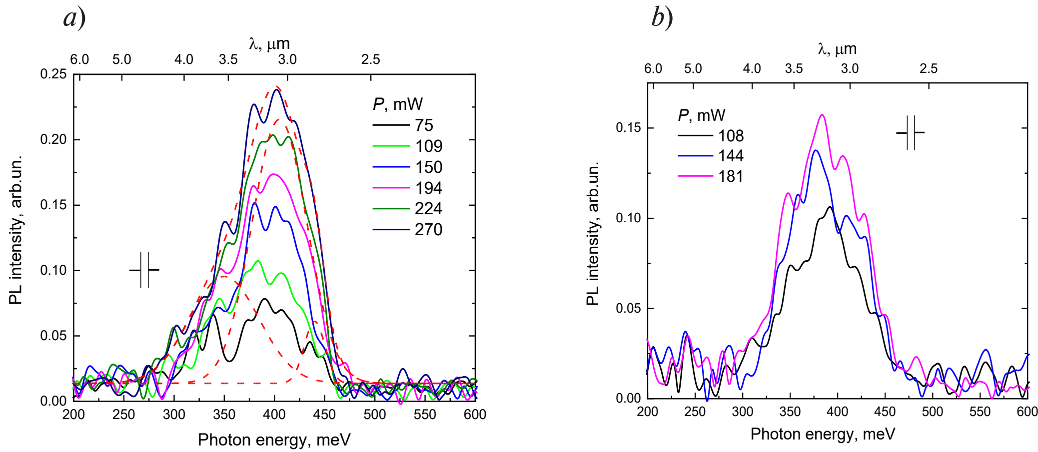

Fig. 3. PL spectra of pure InAs NWs at different pumping levels at 77 K (*a*); PL spectra of the thinner pure InAs NWs with low surface concentration (*b*)

Photoluminescence spectra of InAs-core/CaF_2-shell NWs (not shown here) demonstrated the same peak positions as it was observed in pure InAs NWs. The dependencies on temperature and pumping intensity also were the same. This indicates that the passivating CaF_2 layer is amorphous and does not affect the band structure of InAs NWs.

Photoluminescence spectra of InAs-core / InP-shell NWs are presented in Fig. 4, *a* for different pumping levels for NWs with thin shell. Interband PL peak position is about 445 meV, which corresponds to the direct carrier transitions in the wurtzite phase. The PL intensity of core/shell NWs is 2–3 times higher than intensity of pure NWs. The interband PL peak of InAs-core / InP-shell NWs with thick shell was observed at the photon energy about 480 meV (see Fig. 4, *b*). Thus, we can conclude that the InP shell over the InAs NWs provides a significant increase of *Eg*. It can be explained by deformation of the NW core lattice due to compression by the shell. Increasing the shell of NW causes the higher deformation and corresponding higher *Eg* (see blueshift of PL peak presented in Fig. 4, *b*). It is important to note that due to the passivation of the NW surface, not only the blue shift of the peak was occurred, but also, we observed an increase in its intensity. Additionally, it should be noted that longwavelength PL peak corresponded to indirect transitions has retained its position in coated NWs. It could be explained by the absence of the influence of passivation on the *Eg* of zincblende.

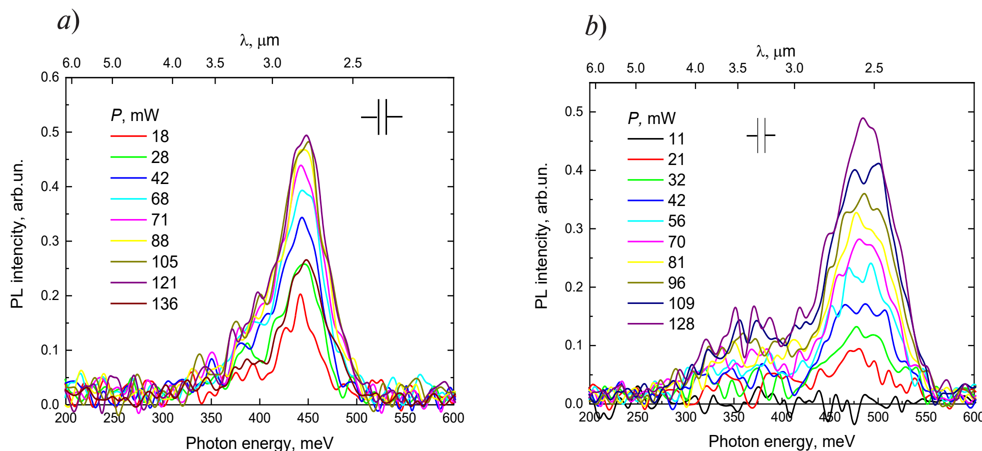

Fig. 4. PL spectra of InAs-core / InP-shell NWs with thick (*a*) and thin (*b*) shell at different pumping levels at the temperature of 77 K

Conclusion

Polytypism of InAs nanowires was found and proved by TEM and the measurements of interband PL spectra in the infrared spectral range. The positions of the PL peaks agree with the theoretical calculations of other authors. Also, it has been shown that InP passivation of InAs nanowires results in a blue shift of interband transitions due to the mechanical strain caused by the shell. The PL intensity of core/shell NWs exceeds the PL intensity of pure InAs NWs.

Acknowledgments

This work was supported by the Russian Science Foundation (grant № 22-19-00494, https://rscf.ru/en/project/22-19-00494/). TEM characterizations were performed using equipment of the Federal Joint Research Center "Material science and characterization in advanced technology" supported by the Ministry of Science and Higher Education of the Russian Federation (id RFMEFI62117X0018)

REFERENCES

1. **Xu T., Wang H., Chen X., Luo M., Zhang L., Wang Y., Chen F., Shan C., Yu C.,** Recent progress on infrared photodetectors based on InAs and InAsSb nanowires, Nanotechnology. 31 (2020) 294004.
2. **Zhang Y., Wu J., Aagesen M. Liu H.,** III—V nanowires and nanowire optoelectronic devices, Journal of Physics D: Applied Physics. 48 (2015) 463001.
3. **Jurczak P., Zhang Y., Wu J., Sanchez A.M., Aagesen M., Liu H.,** Ten-fold Enhancement of InAs Nanowire Photoluminescence Emission with an InP Passivation Layer, Nano letters. 17 (6) (2017) 3629–3633.
4. **Dayeh S.A.,** Electron transport in indium arsenide nanowires, Semiconductor Science and Technology. 25 (2010) 024004.
5. **Sun M.H., Joyce H.J., Gao Q., Tan H.H., Jagadish C., Ning C.Z.,** Removal of Surface States and Recovery of Band-Edge Emission in InAs Nanowires through Surface Passivation Nano letters. 12 (7) (2012) 3378–3384.
6. **Pournia S., Linser S., Jnawali G., Jackson H.E., Smith L.M., Ameruddin A., Caroff P., Wong-Leung J., Tan H.H., Jagadish C., Joyce H.J.,** Exploring the band structure of Wurtzite InAs nanowires using photocurrent spectroscopy, Nano Research. 13 (6) (2020) 1568–1591.
7. **De A., Pryor C.E.,** Predicted band structures of III-V semiconductors in the wurtzite phase, Physical Review B. 81 (15) (2010) 155210.
8. **Faria Junior P.E., Campos T., Bastos C.M.O., Gmitra M., Fabian J., Sipahi G.M.,** Realistic multiband k · p approach from *ab initio* and spin-orbit coupling effects of InAs and InP in wurtzite phase, Physical Review B. 93(23) (2016) 234204.
9. **Logeeswaran V.J., Oh J., Nayak A.P., Katzenmeyer A.M., Gilchrist K.H.,** A perspective on nanowire photodetectors: current status, future challenges, and opportunities, IEEE Journal of selected topics in quantum electronics. 17 (4) (2011) 1002–1032.
10. **Svensson J., Anttu N., Vainorius N., Borg B. M., Wernersson L.-E.,** Diameter-dependent photocurrent in InAsSb nanowire infrared photodetectors, Nano letters. 13 (4) (2013) 1380–1385.
11. **Rota M.B., Ameruddin A.S., Fonseka H.A., Gao Q., Mura F., Polimeni A., Miriametro A., Tan H.H., Jagadish C., Capizzi M.,** Bandgap Energy of Wurtzite InAs Nanowires, Nano Letters. 16 (8) (2016) 51917–5203.
12. **Möller M., de Lima Jr. M.M., Cantarero A., Chiaramonte T., Cotta M.A. Iikawa F.,** Optical emission of InAs nanowires, Nanotechnology. 23 (2012) 375704.

THE AUTHORS

USTIMENKO Ratmir V.
ratmirustimenko@yandex.ru
ORCID: 0000-0003-4123-4375

VINNICHENKO Maksim Ya.
mvin@spbstu.ru
ORCID: 0000-0002-6118-0098

KARAULOV Danila A.
karaulov.da@edu.spbstu.ru

FIRSOV Dmitry A.
dmfir@rphf.spbstu.ru
ORCID: 0000-0003-3947-4994

FEDOROV Vladimir V.
burunduk.uk@gmail.com
ORCID: 0000-0001-5547-9387

Mozharov Alexey M.
alex000090@gmail.com
ORCID: 0000-0002-8661-4083

Kirilenko Demid A.
zumsisai@gmail.com
ORCID: 0000-0002-1571-209X

Mukhin Ivan S.
imukhin@yandex.ru
ORCID: 0000-0001-9792-045X

Received 30.11.2022. Approved after reviewing 08.12.2022. Accepted 15.12.2022.

© Peter the Great St. Petersburg Polytechnic University, 2023